

Swift heavy ion induced surface and microstructural evolution in metallic glass thin films

Hysen Thomas^{a,1,*}, Senoy Thomas^{a,2}, Raju V. Ramanujan^b, D.K. Avasthi^c, I.A. Al-Omari^d, Salim Al-Harhi^d, M.R. Anantharaman^{a,*}

^a Department of Physics, Cochin University of Science and Technology, Cochin 682 022, Kerala, India

^b School of Materials Engineering, Nanyang Technological University, Nanyang Avenue 639 798, Singapore

^c Inter University Accelerator Centre, Aruna Asaf Ali Marg, New Delhi 110 067, India

^d Department of Physics, Sultan Qaboos University, Al Khoud, Muscat, Oman

ARTICLE INFO

Article history:

Received 28 January 2012

Received in revised form 22 May 2012

Available online 7 June 2012

Keywords:

Swift Heavy Ion

AFM

PSD

SPIP

Magnetic Thin Films

ABSTRACT

Swift heavy ion induced changes in microstructure and surface morphology of vapor deposited Fe–Ni based metallic glass thin films have been investigated by using atomic force microscopy, X-ray diffraction and transmission electron microscopy. Ion beam irradiation was carried out at room temperature with 103 MeV Au⁹⁺ beam with fluences ranging from 3×10^{11} to 3×10^{13} ions/cm². The atomic force microscopy images were subjected to power spectral density analysis and roughness analysis using an image analysis software. Clusters were found in the image of as-deposited samples, which indicates that the film growth is dominated by the island growth mode. As-deposited films were amorphous as evidenced from X-ray diffraction; however, high resolution transmission electron microscopy measurements revealed a short range atomic order in the samples with crystallites of size around 3 nm embedded in an amorphous matrix. X-ray diffraction pattern of the as-deposited films after irradiation does not show any appreciable changes, indicating that the passage of swift heavy ions stabilizes the short range atomic ordering, or even creates further amorphization. The crystallinity of the as-deposited Fe–Ni based films was improved by thermal annealing, and diffraction results indicated that ion beam irradiation on annealed samples results in grain fragmentation. On bombarding annealed films, the surface roughness of the films decreased initially, then, at higher fluences it increased. The observed change in surface morphology of the irradiated films is attributed to the interplay between ion induced sputtering, volume diffusion and surface diffusion.

© 2012 Elsevier B.V. All rights reserved.

1. Introduction

Metallic amorphous alloys are a class of materials that are widely investigated for plausible technological applications; owing to their enhanced structural, magnetic and electrical properties [1–4]. Most of these outstanding properties can be attributed to their random crystalline structure [3]. These materials can be synthesized by a variety of techniques like physical vapor deposition, solid-state reaction, ion beam irradiation, melt spinning, and mechanical alloying [3,4], of which, ion beam irradiation seems to be a promising technique since it can induce a variety of changes

in the material ranging from bulk structural to local magnetic properties. During irradiation, swift heavy ions (SHI) passing through a material with velocities comparable to the Bohr velocity of electrons, lose energy mainly by two processes, namely, nuclear energy loss, and electronic energy loss. The former is dominant when the ion energy is in the keV range, and latter is dominant when the ion energy is in the MeV range.

Most of the effects associated with SHI irradiation occur in the electronic energy loss regime. This inelastic scattering assisted energy loss of fast heavy ions creates latent tracks, phase transitions, amorphization, damage creation, annealing effects, dimensional changes, and nanostructures. During irradiation, the surface morphology also evolves resulting from the competition between dynamic roughening; which increases the surface roughness, and smoothening which decreases it. Recently, A. Kanjilal and D. Kanjilal [5] reported surface roughening kinetics of 100 MeV Au beam irradiated Si_{1-x}Ge_x alloy films for $x = 0.5$ and 0.7. The irradiation induced surface roughening behavior is demonstrated by studying the variation of surface roughness as a function of fluence. The composition

* Corresponding authors.

E-mail addresses: hysenthomas@gmail.com (H. Thomas), mraiyer@gmail.com (M.R. Anantharaman).

¹ On Deputation from Department of Physics, Christian College, Angadical, Chengannur – 689 122, Kerala, India. Tel.: +91 9446974398.

² Present address: Institute of Physics, Chemnitz University of Technology, 09107 Chemnitz, Germany.

dependent variation of surface morphology with increasing fluence is ascribed to the strain distribution along the sample surface. Thomas et al. [6] reported SHI irradiation induced coercivity changes in Fe–Ni based thin films and the observed changes were correlated with topographical evolution of the films with fluence. Dash et al. [7] carried out quantitative roughness and microstructure analysis of as-deposited and SHI (107 MeV Ag and 58 MeV Ni) irradiated 10 and 20 nm thick Au films using AFM and its power spectral density analysis. They reported an increase in the root mean square (rms) roughness at low fluences and a decrease at higher fluences. The PSD analysis also showed similar variation of low frequency roughness with ion fluence. In the high frequency regime, surface morphology of irradiated samples was found to be governed by a combined effect of evaporation–re-condensation and diffusion dominated processes. Gupta and Avasthi [8] reported sputtering in Au thin films, resulting from energy deposition in the films, owing to inelastic collision of SHI with electron clouds of target atoms. Gupta et al. [9] reported SHI induced surface smoothing, roughening and sputtering of thermally immiscible Fe/Bi bilayer system. The observed behavior of surface smoothing and roughening under SHI irradiation was explained on the basis of the thermal spike model. In general, magnetic properties of thin films are sensitively correlated to the surface roughness and hence it will be worthwhile to probe possible mechanisms by which roughness of thin films can be tailored. Further, rough films can act as templates for the growth of nanostructures using oblique angle deposition [10]. Pre-patterned substrates offer a suitable platform for growth of nanostructures by suitable deposition techniques.

There are also reports that electronic energy transfer to the amorphous alloys can lead to anisotropic growth, which means, shrinkage of alloy ribbons in the direction of the beam and expansion in the direction transverse to it [11]. In thin films, this type of effects can create large stress in the film–substrate interfacial boundaries. The dense random arrangement of atoms in metallic glasses favors amorphous structure due to the increased liquid–solid interfacial energy. Any structural or morphological changes occurring in these materials are of great importance in determining the magnetic properties. Hence, amorphous alloys can serve as ideal templates to investigate these varied effects.

Scanning probe microscopy (SPM) is a versatile technique to probe surface morphology of thin films in the nano range. In case of magnetic thin films, surface morphology from AFM and magnetic morphology from magnetic force microscopy (if there is considerable out-of-plane stray field) can be extracted employing specific tips in SPM. The images can be further subjected to Fourier analysis using image analysis software to obtain PSD, roughness and auto correlation functions.

Most of the available literatures pertaining to the study of material modification by ion beams were based on bulk materials. Work on metallic glass thin films based on iron and nickel is seldom reported [12–16]. The authors group recently reported 108 MeV Ag^{8+} ions induced surface modification of Fe–Ni based metallic glass thin films in the as-deposited state [6]. In the present investigation, we focus on the influence of swift heavy ions on the microstructure and surface morphology of 673 K annealed metallic glass thin films, so as to study the impact of SHI on the crystalline nature of these films. The results are correlated with a view to gain insight into the structural and morphology evolution with SHI irradiation.

2. Experimental

2.1. Thin film preparation

Metglas thin films with nominal thickness of 100 nm were vacuum evaporated using tungsten filaments on chemically and

ultrasonically cleaned glass substrates from a composite target having composition $\text{Fe}_{40}\text{Ni}_{38}\text{B}_{18}\text{Mo}_4$. The chamber pressure before deposition was 1×10^{-6} mbar, which increased to 3×10^{-5} mbar during deposition. We recently studied the microstructure and magnetic evolution of Fe–Ni based thin films with thermal annealing [12,14]. From the TEM images it was found that, the microstructure of as-deposited films exhibits a contrast typical of an amorphous material [14]. The bright field TEM images of the films annealed at 473, 573 and 673 K, revealed that the microstructure consisted of nanocrystallites embedded in an amorphous phase. Grain growth was also observed with an increase in the annealing temperature [12,14]. Based on those results, the as-deposited Fe–Ni based metallic glass films were annealed at 673 K for 1 h. Annealing was performed at 4×10^{-5} mbar for minimizing surface oxidation.

2.2. Swift heavy ion irradiation

As deposited as well as annealed films were irradiated with 103 MeV Au^{9+} ions at the 15 UD Pelletron accelerator at IUAC, New Delhi. The irradiations were performed at 0° angle of incidence with respect to the surface normal. Ion beam was raster scanned on the sample surface by a magnetic scanner for maintaining a uniform ion flux throughout the film. The fluences were varied from 3×10^{11} to 3×10^{13} ions/cm². The irradiated sample area was 1 cm². The Au ion is chosen due to its higher mass and the energy regime is selected after simulation using SRIM code [17]. For the chosen ion energy of 103 MeV, the lateral straggling is 5.87 μm , longitudinal straggling is 4.62 μm and the penetration depth is 6.98 μm . This value of penetration depth is two orders of magnitude greater than the thickness of the film. The energy of the Au^{9+} beams (103 MeV) was selected with a view to avoid the ion implantations in the film with maximum electronic loss of 39 keV/nm and minimum nuclear energy losses within the accelerators maximum energy limit (see Fig. 1).

The samples were mounted on a massive copper block using carbon tape. The increase in sample temperature during ion irradiation can be estimated using the Fourier heat conduction equation, $j = -\lambda \frac{dT}{dz}$. The total heat carried into the system can be taken as the total energy carried by SHI, $= \phi E_{shi}$, where ϕ is the ion flux and E_{shi} is the ion energy. In this study, a low ion flux of 6×10^9 cm²/s was maintained with energy of 103 MeV per ions. The conductivity of float glass is nearly equal to $1 \text{ W m}^{-1} \text{ K}^{-1}$. However, even if we

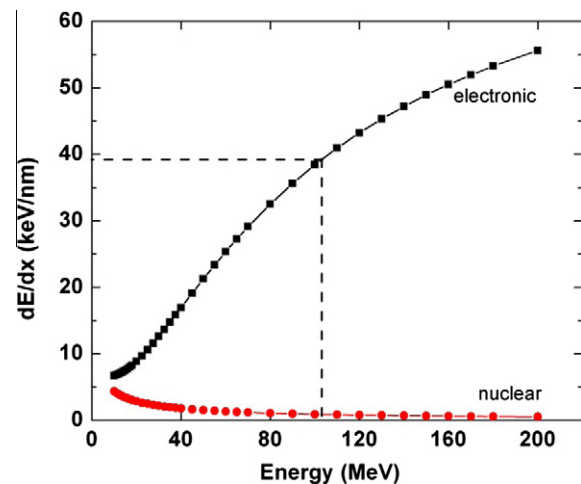


Fig. 1. SRIM simulation showing electronic and nuclear energy loss versus ion energy. Dashed line shows the electronic energy loss corresponding to 103 MeV energy.

assume a very low conductivity for the system of film, glass substrate and carbon tape, the Fourier equation predicts a temperature rise of less than 10 K at the film surface [18,19]. Thus the temperature rise due to ion irradiation is assumed to be small to affect any microstructural changes in the film.

2.3. Characterization

The XRD pattern of all samples were recorded using an X-ray diffractometer (Rigaku D-max-C) using Cu K α radiation ($\lambda = 1.54 \text{ \AA}$). The average particle size is estimated from measured width of the diffraction curves using Debye–Scherrer formula, $D = \left(\frac{0.9\lambda}{\beta \cos\theta}\right)$ where β is full width at half maximum (FWHM), D the average grain size and θ the diffracting angle. The surface topography of all thin films were analyzed using an AFM (Digital Instruments Nanoscope III). The AFM images were analyzed using surface data analysis software SPIP (Image Metrology A/S, Hørsholm, Denmark) to obtain PSD, roughness and auto correlation functions. TEM measurements were performed in a 200 kV Philips CM 20 FEG TEM.

3. Results and discussion

3.1. Microstructural evolution with SHI irradiation

Fig. 2(a) shows XRD pattern of as-deposited Fe–Ni based metallic glass thin film. The film appears to be amorphous in XRD. In order to have a deeper insight into the microstructure of the as-deposited films, high resolution transmission electron microscopy imaging was performed on this sample. Fig. 3(a) shows a HRTEM image collected for the as-deposited sample. It is clear that a short range atomic ordering prevails in the as-deposited samples with crystallites of size around 3 nm embedded in an amorphous matrix. Electron diffraction pattern (Fig. 3(b)) showed diffraction rings corresponding to inter-planar distance $d = 0.254, 0.207$ and 0.146 nm , of which, $d = 0.207 \text{ nm}$ can be attributed to (111) of fcc Fe–Ni. The XRD pattern of Fe–Ni based metallic glass thin film annealed at 673 K is shown in Fig. 2(b). In contrast to the diffraction patterns of the as-deposited thin films, the annealed films clearly indicate improved crystallinity with thermal treatment. From TEM images (Fig. 3(c)), it is clear that the grain growth has occurred on thermal annealing at 673 K. Diffraction pattern

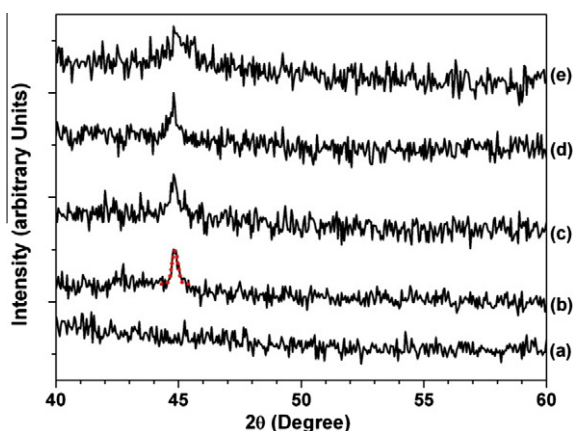


Fig. 2. X-ray diffraction pattern of Fe–Ni based thin films, (a) as-deposited, (b) annealed at 673 K, the red dotted line shows a Gaussian fit to the peak to evaluate the crystallite size, (c) annealed at 673 K and irradiated at fluence $3 \times 10^{11} \text{ ions/cm}^2$, (d) annealed at 673 K and irradiated at fluence $3 \times 10^{12} \text{ ions/cm}^2$ and (e) annealed at 673 K and irradiated at fluence $3 \times 10^{13} \text{ ions/cm}^2$. (For interpretation of the references to colour in this figure legend, the reader is referred to the web version of this article.)

(Fig. 3(d)), depicts rings corresponding to $d = 0.254, 0.207, 0.180, 0.170, 0.152$ and 0.127 nm , of which, $d = 0.207, 0.180$ and 0.127 nm can be attributed to the (111), (002) and (022) of fcc Fe–Ni, respectively. Further experiments are necessary to identify the origin of diffraction ring corresponding to $d = 0.254, 0.170, 0.146$ and 0.152 nm .

SHI irradiation on as-deposited films with fluences ranging from 3×10^{11} to $3 \times 10^{13} \text{ ions/cm}^2$ did not produce any observable changes in the XRD pattern (results not shown). The absence of any observable changes in the XRD pattern with irradiation can be attributed to the fact that the as-deposited films were already in a nanocrystalline state possessing a short range atomic order and the electronic energy loss of swift heavy ions in the material is stabilizing this short range order.

SHI irradiation on thermally annealed films with fluences ranging from 3×10^{11} to $3 \times 10^{13} \text{ ions/cm}^2$ resulted in progressive line broadening of the XRD peak indicating fragmentation of crystallites with ion beam irradiation. The 673 K annealed sample already contains crystallites formed by nucleation and growth due to thermal treatments. Irradiation of these films with higher fluences of SHI leads to size reduction of grains with multiple ion impacts and hence broadening of the peaks were observed (Fig. 1(c–e)). For an approximate estimate of the grain size, the full width at half maximum of the XRD peak was determined from a Gaussian fit. The 673 K annealed sample shows crystalline peak of Fe–Ni and the average crystallite size was estimated to be $28 \pm 3.6 \text{ nm}$. On irradiation of the sample with SHI at a fluence of $3 \times 10^{11} \text{ ions/cm}^2$, the crystallite size reduces to $21 \pm 2.7 \text{ nm}$. The film irradiated at a fluence of $3 \times 10^{12} \text{ ions/cm}^2$ showed crystallites with size $15 \pm 1.9 \text{ nm}$ and at a higher fluence of $3 \times 10^{13} \text{ ions/cm}^2$, the particle size further reduced to $6 \pm 0.77 \text{ nm}$. The reduction in crystallite size as a result of SHI irradiation can be attributed to the strain induced fragmentation of crystallites. So far, thermal spike [20,21] and Coulomb explosion models [22–24] have been successively used to describe the strain in the crystallites due to swift heavy ions. According to thermal spike model, the energy is deposited by the projectile ions in the electronic sub-system of the material. This energy is shared among the electrons by electron–electron coupling and is transferred subsequently to the lattice atoms via electron–lattice interactions. This results in a large increase in the temperature along and in the vicinity of the ion path. Because of the temperature spike, pressure waves will develop and causes strain in the crystallites. On the other hand, according to the Coulomb explosion model, a highly ionized zone of charged particles is created along the ion path. The ionization zone with positive charges may explode under electrostatic force and induces strain in the material. This strain may lead to the fragmentation of crystallites.

However, in addition to the crystallite size reduction, a partial contribution of the atom dislocations to the XRD line broadening also cannot be ruled out.

3.2. Surface evolution with ion beam irradiation

Fig. 4(a) shows AFM image of a Fe–Ni based metallic glass thin film annealed at 673 K. Lateral structures of sizes around 30 nm can be observed. From the AFM images shown in Fig. 4(b–d), it is clear that irradiation of these annealed films, with 103 MeV Au⁹⁺ ions, changes the surface morphology, first at $3 \times 10^{11} \text{ ions/cm}^2$, smoothing of the mesoscopic hill-like structures take place, and then, at $3 \times 10^{12} \text{ ions/cm}^2$, new surface structures are created, and at still higher doses of $3 \times 10^{13} \text{ ions/cm}^2$, an increase in the surface roughness is observed.

The evolution of surface roughness of the annealed films, irradiated at various fluences is shown in Fig. 5. The average roughness (S_a) of the 673 K annealed films is 27.05 nm and root mean square

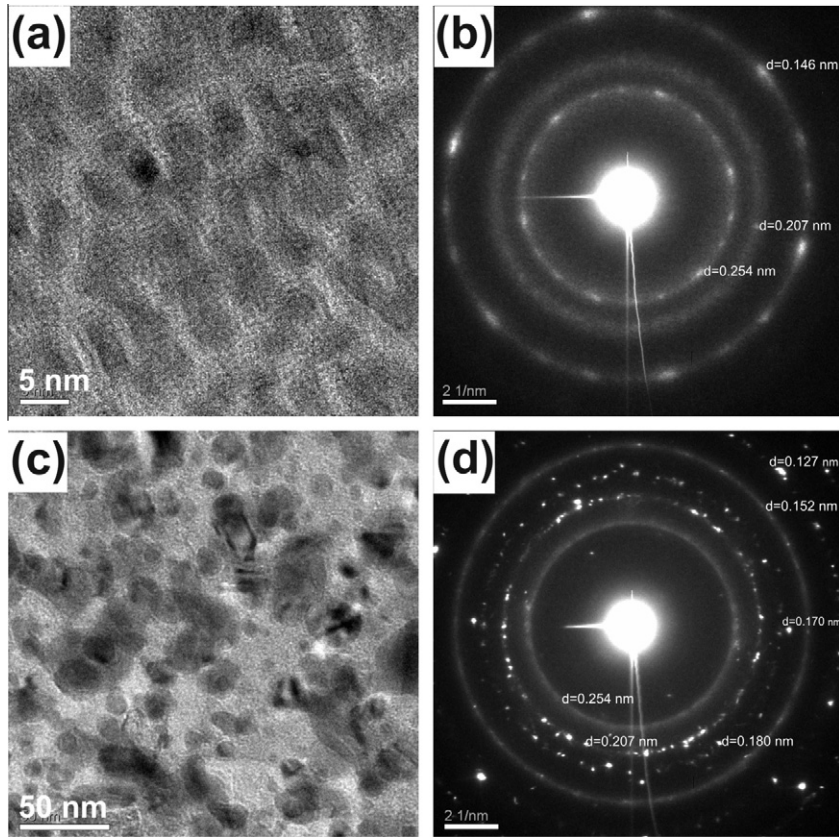


Fig. 3. (a) HRTEM image and (b) electron diffraction pattern of as-deposited Fe–Ni based metallic glass thin film, (c) TEM bright field image and (d) electron diffraction pattern of Fe–Ni based metallic glass thin film after annealing at 673 K for 1 h.

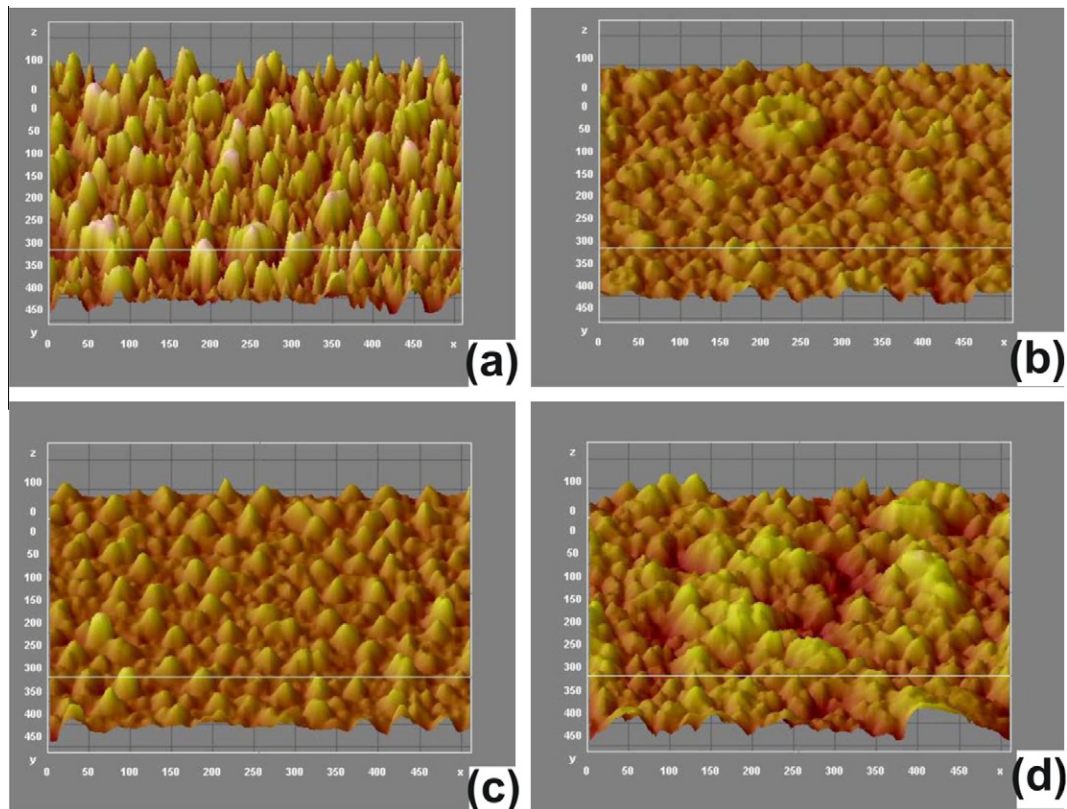


Fig. 4. 3D AFM images of Fe–Ni based metallic glass thin films (a) annealed at 673 K and subsequently irradiated with 103 MeV Au^{9+} ions of fluence, (b) $3 \times 10^{11} \text{ ions/cm}^2$, (c) $3 \times 10^{12} \text{ ions/cm}^2$ and (d) $3 \times 10^{13} \text{ ions/cm}^2$. Image size is 500 nm^2 and z scale is 100 nm.

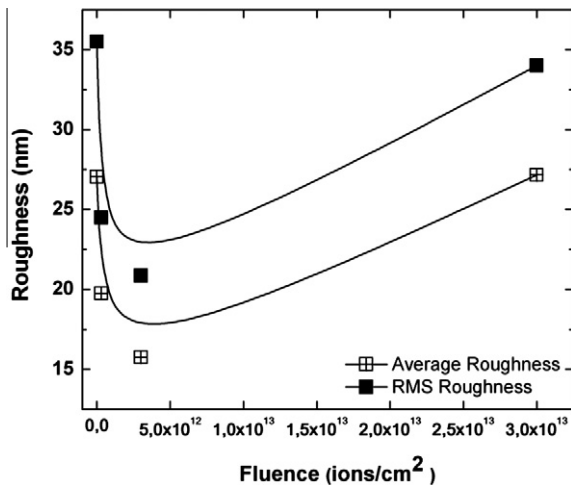


Fig. 5. Variation of surface roughness with ion fluence. Solid line is drawn as a guide to eye.

roughness (S_q) is 35.51 nm. However, on SHI irradiation roughness of the films reduces to value 19.75 and 24.49 nm (S_a , S_q) at fluences 3×10^{11} ions/cm² and 15.74, 20.85 nm (S_a , S_q) at 3×10^{12} ions/cm² and thereafter monotonically increases to 27.16 and 34.01 nm (S_a , S_q). The rapid initial decrease in surface roughness with ion fluence indicates that a surface smoothing process is taking place in the sample for the initial fluences. Plausible origins of this surface smoothing can be irradiation induced viscous flow, volume diffusion, or surface diffusion. Mayr and Averback [25] also observed surface smoothing in ion irradiated films. They identified smoothing process using stochastic rate equations for the evolution of the surface in Fourier space. In their example, they attributed the smoothing predominantly to irradiation-induced viscous flow. Goswami and Dev [26] observed a surface smoothing in silicon surfaces irradiated by a 2-MeV Si⁺ ion beam. They explained the origin of irradiation induced surface smoothing as follows. The collision cascade as a result of ion–solid interaction can enable target atoms to acquire a kinetic energy enough to escape from the solid surface (sputtering). However, if the energy (component normal to surface) of the displaced atoms is smaller than the surface binding energy, the atoms may reach the surface but cannot leave the surface. They can, however, drift parallel to the surface. Surface smoothing originates because of those atoms, which are ejected from the surface with too low energy to escape the energy barrier, but can translate parallel to the surface.

In order to have a deeper understanding on the initial surface smoothing mechanism with ion beam irradiation, power spectral density was obtained from the AFM images. The power spectral density of the films is shown in Fig. 6.

From the log–log plot of PSD spectrum two different regions are visible. The low spatial frequency region (region I) corresponds to the uncorrelated white noise and the high frequency region (region II) represents correlated surface features. The PSD curves of the un-irradiated and irradiated films extracted from the AFM images essentially present the same characteristic features consisting of a gradient in the high spatial frequency region and a low frequency region separated by a small cross over region. The slope of the high frequency region of the PSD curves is intimately connected to the kinetics of surface evolution and hence can suggest the predominant mechanism responsible for the surface evolution of thin films with SHI. The variation in the slope of the high frequency region of the PSD curve is shown in Fig. 7.

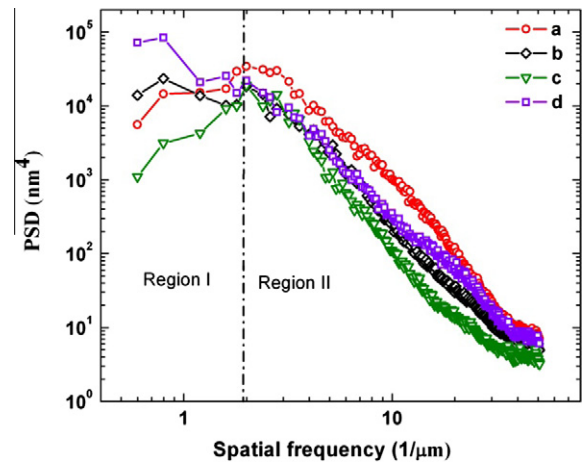


Fig. 6. Power spectral density plots of Fe–Ni based metallic glass thin films (a) annealed at 673 K and subsequently irradiated with 103 MeV Au⁹⁺ ions of fluence, (b) 3×10^{11} ions/cm², (c) 3×10^{12} ions/cm² and (d) 3×10^{13} ions/cm².

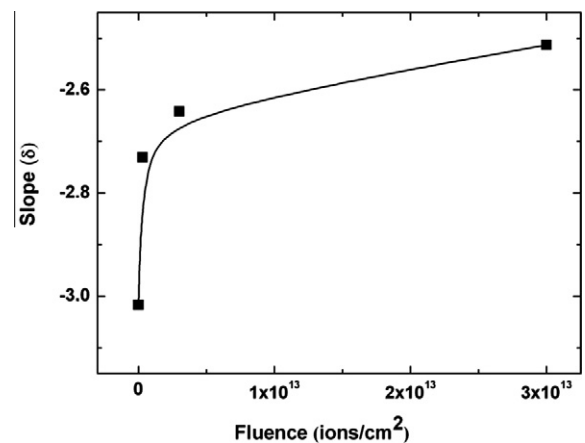


Fig. 7. Dependence of the slope of the PSD spectrum (region II) with different ion fluences. Solid line is drawn as a guide to eye.

It is clear that the slope, δ , gradually increases up to 3×10^{12} ions/cm² and thereafter the change in slope is relatively small. Earlier works by Herring and Mullins [27–29] established δ values of 1, 2, 3, and 4 to four different surface transport mechanisms, i.e., plastic flow driven by surface tension, evaporation and recondensation of particles, volume diffusion, and surface diffusion, respectively. It is to be noted that, the evolution of surface morphology of solids during ion beam irradiation is governed by the interplay between the dynamics of surface roughening that occurs during sputtering and smoothing induced by the material transport. From Fig. 7 and comparing δ values with that suggested in the previous works, it is evident that as the irradiation fluence increases, the dominant material transport mechanism changes from volume diffusion to evaporation–condensation. This also explains the increased surface roughness at higher irradiation fluence. Surface roughening is assumed to be because of the evaporation of atoms from a hot surface heated by an inelastic thermal spike. The results indicate that at higher fluence 3×10^{13} ions/cm², the surface evaporation mechanism (sputtering) results in an increase in surface roughness and this is in line with our previous observations in 108 MeV Ag⁸⁺ ion irradiated, as-deposited Fe–Ni based thin films [6].

From the combined XRD and AFM investigations it is seen that SHI is effective in surface modification of Fe–Ni based metallic

glass thin films. However, further experiments are necessary to optimize these effects for specific applications.

4. Conclusions

Fe–Ni based metallic glass thin films were prepared by thermal evaporation. The films were annealed at 673 K and show more crystallinity than the as-deposited films. The as-deposited and annealed films were subjected to SHI irradiation at various fluences and their structural and morphological properties were investigated. The absence of any observable changes in the XRD of as-deposited films with ion beam irradiation can be attributed to the fact that the as-deposited films were already with a short range atomic order and the ion irradiation is stabilizing this short range order. For samples annealed at 673 K, upon irradiation, a significant reduction in grain size with ion fluence is observed. The grain fragmentation during ion beam irradiation is attributed to the strain transferred to the crystallites by the electronic energy loss. The irradiation of the sample rapidly changes the surface topography, first at 3×10^{11} ions/cm² smoothing of the mesoscopic hill-like structures, and then at 3×10^{12} ions/cm², creation of surface structures and at still higher doses of 3×10^{13} ions/cm² an increase in the roughness is observed. Volume diffusion was identified as the prominent surface smoothening mechanism at lower ion fluences and at higher fluences surface roughening was observed. Further investigations regarding the interplay between surface morphology and magnetic properties in these thin films are going on and there exists ample scope for probing the evolution of magnetic properties with surface morphology in the case of magnetic films.

Acknowledgements

M.R.A. and H.T. acknowledge Inter University Accelerator Centre, New Delhi for providing financial assistance in the form of a project. H.T. acknowledges financial assistance received from UGC-FDP, India & DST FIST project received by Department of Physics, Christian College, Chengannur, Kerala, India. The author's acknowledge B. Mainz (TU Chemnitz) for TEM measurements. I.A. Al-Omari is grateful to Sultan Qaboos University for the support provided to perform this study under the research Grant, number IG/SCI/PHYS/12/02. M.R.A. acknowledges the support received through the DST-DAAD exchange programme.

References

- [1] Mark Telford, The case for bulk metallic glass, *Mater. Today* 7 (2004) 36.
- [2] W. Klement Jr., R.H. Willens, P. Duwez, Non-crystalline structure in solidified gold–silicon alloys, *Nature* 187 (1960) 869.
- [3] M.E. McHenry, M.A. Willard, D.E. Laughlin, Amorphous and nanocrystalline materials for applications as soft magnets, *Prog. Mater. Sci.* 44 (1999) 291.
- [4] T. R. Anantharaman, *Metallic Glasses: Production, Properties and Applications* Trans Tech Publications, Switzerland, 1984.
- [5] A. Kanjilal, D. Kanjilal, Surface roughening in Si_{1-x}Ge_x alloy films by 100 MeV Au: composition dependency, *Solid State Commun.* 139 (2006) 531.
- [6] Senoy Thomas, Hysen Thomas, D.K. Avasthi, A. Tripathi, R.V. Ramanujan, M.R. Anantharaman, Swift heavy ion induced surface modification for tailoring coercivity in Fe–Ni based amorphous thin films, *J. Appl. Phys.* 105 (2009) 033910.
- [7] P. Dash, P. Mallick, H. Rath, A. Tripathi, Jai Prakash, D.K. Avasthi, S. Mazumder, S. Varma, P.V. Satyam, N.C. Mishra, Surface roughness and power spectral density study of SHI irradiated ultra-thin gold films, *Appl. Surf. Sci.* 256 (2009) 558.
- [8] A. Gupta, D.K. Avasthi, Large electronically mediated sputtering in gold films, *Phys. Rev. B* 64 (2001) 155407.
- [9] A. Gupta, R.S. Chauhan, D.C. Agarwal, S. Kumar, S.A. Khan, A. Tripathi, D. Kabiraj, S. Mohapatra, T. Som, D.K. Avasthi, Smoothing, roughening and sputtering: the complex evolution of immiscible Fe/Bi bilayer system, *J. Phys. D: Appl. Phys.* 41 (2008) 215306.
- [10] M.M. Hawkeye, M.J. Brett, Glancing angle deposition: fabrication, properties, and applications of micro- and nanostructured thin films, *J. Vac. Sci. Technol. A* 25 (2007) 1317.
- [11] Ming-dong Hou, S. Klaumünzer, G. Schumacher, Dimensional changes of metallic glasses during bombardment with fast heavy ions, *Phys. Rev. B* 41 (1990) 1144.
- [12] T. Hysen, S. Deepa, S. Saravanan, R.V. Ramanujan, D.K. Avasthi, P.A. Joy, S.D. Kulkarni, M.R. Anantharaman, Effect of thermal annealing on Fe₄₀Ni₃₈B₁₈Mo₄ thin films: modified Herzer model for magnetic evolution, *J. Phys. D: Appl. Phys.* 39 (2006) 1993.
- [13] M. Jyothi, C. Suryanarayana, Structure of vapour deposited METGLAS 2826 MB films, *Z. Metallkunde* 76 (1985) 802.
- [14] S. Thomas, S.H. Al-Harhi, D. Sakthikumar, I.A. Al-Omari, R.V. Ramanujan, Y. Yoshida, M.R. Anantharaman, Microstructure and random magnetic anisotropy in Fe–Ni based nanocrystalline thin films, *J. Phys. D: Appl. Phys.* 41 (2008) 155009.
- [15] S. Thomas, S.H. Al-Harhi, R.V. Ramanujan, Zhao Bangchuan, Liu Yan, Wang Lan, M.R. Anantharaman, Surface evolution of amorphous nanocolumns of Fe–Ni grown by oblique angle deposition, *Appl. Phys. Lett.* 94 (2009) 063110.
- [16] S. Thomas, S.H. Al-Harhi, I.A. Al-Omari, R.V. Ramanujan, M.R. Anantharaman, Influence of substrate topography on the growth and magnetic properties of obliquely deposited amorphous nanocolumns of Fe–Ni, *J. Phys. D: Appl. Phys.* 42 (2009) 215005.
- [17] J.F. Ziegler, J.P. Biersack, U. Littmark, *The Stopping and Range of Ions in Solids*, Pergamon, New York, 1985.
- [18] Tobias Röllner, Wolfgang Bolse, Oxygen diffusion and oxide phase formation in iron under swift heavy ion irradiation, *Phys. Rev. B* 75 (2007) 054107.
- [19] P. Mallick, F. Chandana Rath, Jai Prakash, D.K. Mishra, R.J. Choudhary, D.M. Phase, A. Tripathi, D.K. Avasthi, D. Kanjilal, N.C. Mishra, Swift heavy ion irradiation induced modification of the microstructure of NiO thin films, *Nucl. Instrum. Methods Phys. Res. B* 268 (2010) 1613.
- [20] M. Toulemonde, C. Dufour, E. Paumier, Transient thermal process after a high-energy heavy-ion irradiation of amorphous metals and semiconductors, *Phys. Rev. B* 46 (1992) 14362.
- [21] Z.G. Wang, C. Dufour, E. Paumier, M. Toulemonde, The Se sensitivity of metals under swift-heavy-ion irradiation: a transient thermal process, *J. Phys.: Condens. Matter* 6 (1994) 6733.
- [22] E.M. Bringa, R.E. Johnson, Coulomb explosion and thermal spikes, *Phys. Rev. Lett.* 88 (2002) 165501.
- [23] R.L. Fleischer, P.B. Price, R.M. Walker, E.L. Hubbard, Criterion for registration in dielectric track detectors, *Phys. Rev.* 156 (1967) 353–355.
- [24] R.L. Fleischer, P.B. Price, R.M. Walker, Ion explosion spike mechanism for formation of charged-particle tracks in solids, *J. Appl. Phys.* 36 (1965) 3645.
- [25] S.G. Mayr, R.S. Averback, Surface smoothing of rough amorphous films by irradiation-induced viscous flow, *Phys. Rev. Lett.* 87 (2001) 196106.
- [26] D.K. Goswami, B.N. Dev, Nanoscale self-affine surface smoothing by ion bombardment, *Phys. Rev. B* 68 (2003) 033401.
- [27] C. Herring, Effect of change of scale on sintering phenomena, *J. Appl. Phys.* 21 (1950) 301.
- [28] William W. Mullins, Flattening of a Nearly Plane Solid Surface due to Capillarity, *J. Appl. Phys.* 30 (1959) 77.
- [29] William M. Tong, R. Stanley Williams, Kinetics of surface growth: phenomenology, scaling, and mechanisms of smoothening and roughening, *Annu. Rev. Phys. Chem.* 45 (1994) 401.